Development and Application of Weld Track Thermal Analysis for the Exploration Extravehicular Mobility Unit

Christapher Lang[1], Elora Kurz[1], Brian Taminger[2], Bryan Koscielny[2]
[1]NASA Langley Research Center, Hampton, VA
[2]Analytical Mechanics Associates, Inc., Hampton, VA

Worldwide Advanced Manufacturing Symposium
February 22, 2024

Overview

- Introduction
- Thermal Model
- Process Induced Preheat Definition
- Results
  - Racetrack, T-track, Backplate with All Weld Tracks
  - Process Induced Preheat and Melt Pool Width and Depth
  - Validation with Experiment
- Concluding Remarks

Introduction

- Exploration Extravehicular Mobility Unit (xEMU)
  - Next generation spacesuit with improved robustness, inherent redundancy, and increased mobility
  - Designed for use in cislunar space and the lunar surface
  - Developed for the Artemis program
- Exploration Portable Life Support System (xPLSS)
  - Backplate for subsystem assemblies
  - Embedded fluid channels

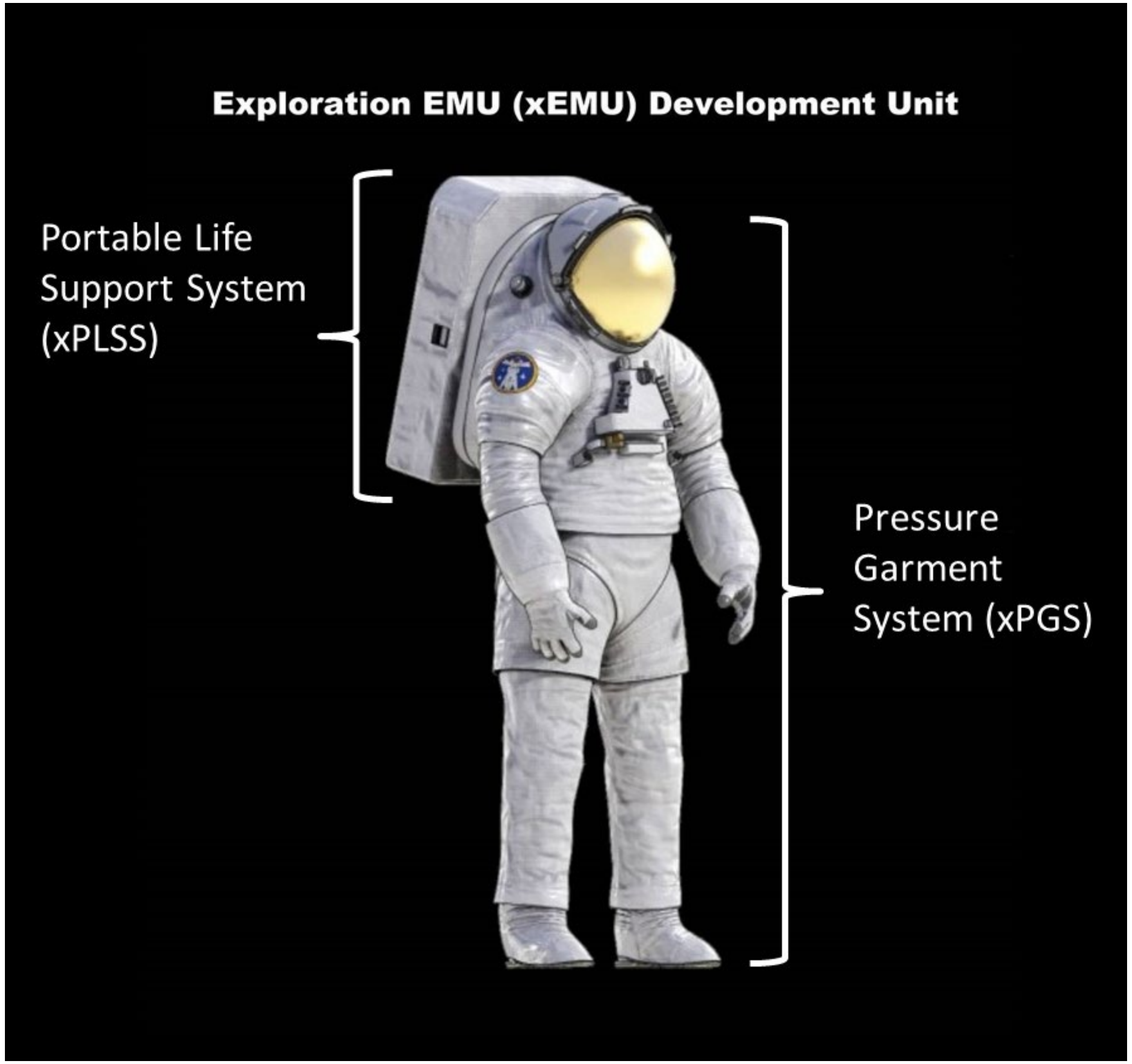

Introduction

- Ti-6Al-4V backplate contains multiple embedded cooling channels
  - Channels are machined out and cover plates are welded onto the channels using an electron beam welder
  - Careful control of the weld process is necessary to completely seal cover plates and produce consistent weld tracks
- Transient finite element analyses were developed to provide support for choosing and controlling weld process parameters to maintain a consistent melt pool around each of the ten weld tracks

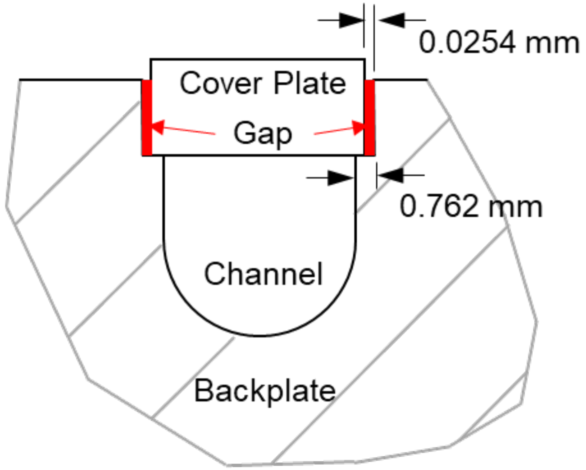

Cross-section diagram of channel and cover plate geometry

Channels with welded cover plates

Electron Beam Weld Background

- Sciaky VX.4-108x78x100 electron beam welder
- All autogenous welds, no filler wire
- Weld path programming compared against quality assurance data
- Low power beam used to precision align the channels to the electron beam welder axes
- Electron beam welds used for tack and full penetration welds
- Weld start/stop sequence performed along weld seam

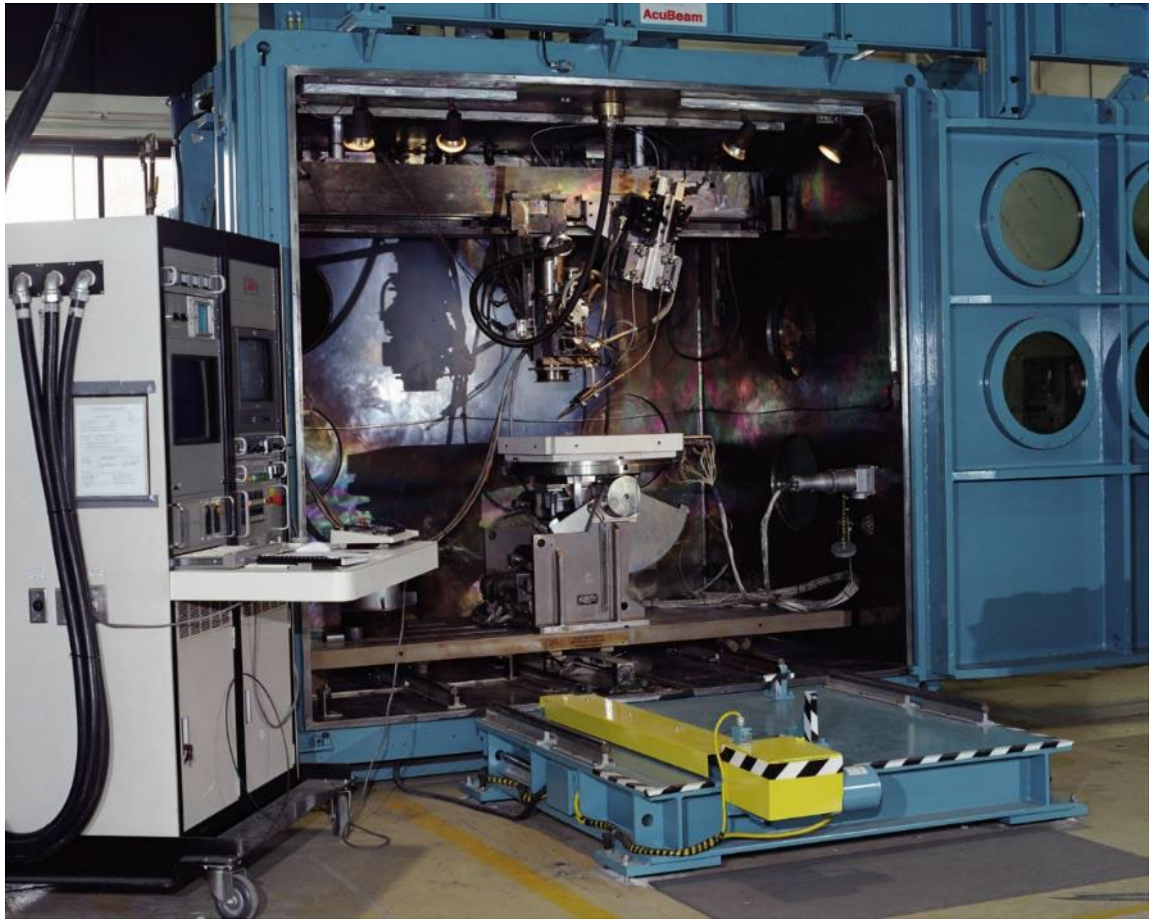

Sciaky electron beam welder at NASA LaRC

Thermal Model

- Transient heat diffusion

$$\rho c_p \frac{\partial T}{\partial t} - \nabla \cdot (k \nabla T) = S_p + S_b$$

  - Energy absorbed and released due to phase change

$$S_p = -\rho L_f \frac{\partial f_L}{\partial t}$$

  - Energy input from the electron beam

$$S_b = \begin{cases} f_1 S_1, & y \le y_e \\ f_2 S_2, & y > y_e \end{cases}$$

  - Boundary conditions

$(k\nabla T) \cdot n = \sigma\epsilon(T^4 - {T_{ref}}^4)$, on top surface

$T = T_B$, on bottom surface

$(k\nabla T) \cdot n = 0$, on all other surfaces

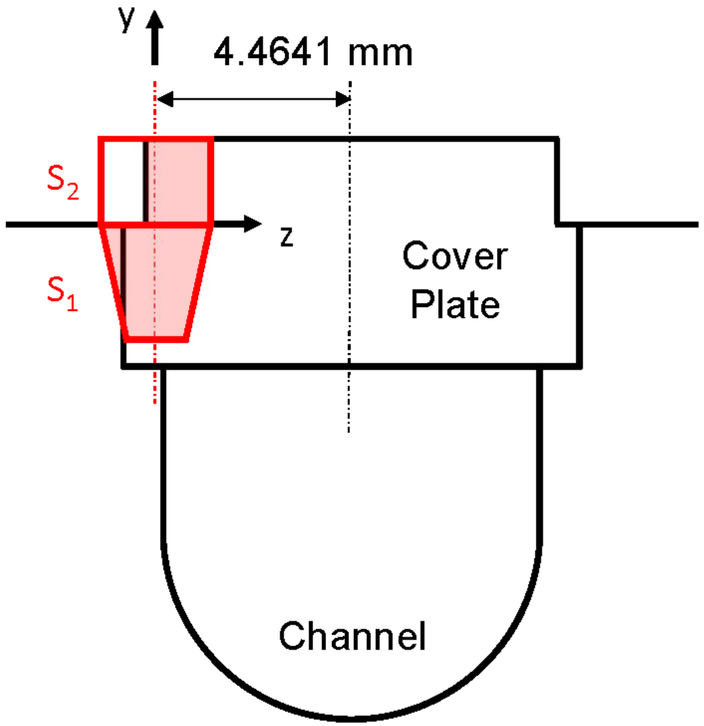

Heat source location with S_1 and S_2 denoted in red

V_1 and V_2 are the volumes defined by the intersection of S_1 and S_2 with the backplate and cover plate respectively

S_2:

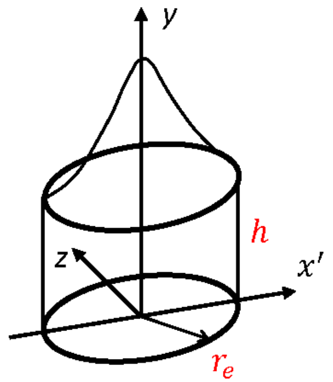

$$f_2 = \frac{V_2}{V_1 + V_2} \frac{Pa}{\int S_2 dV_2}$$

S_1:

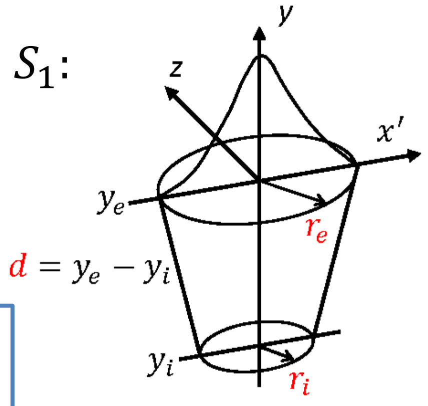

$$f_1 = \frac{V_1}{V_1 + V_2}$$

Heat Source Volume Fraction Correction

- The total energy input, Q_{total}, is known

Power = 1420 W
Absorptivity = 0.95
Q_{total} = 1349 W

- Q_{total} is computed from the heat source distribution

$$Q_{total} = \int S_b dV$$

- Q_{total} was inaccurate and inconsistent at the turn-arounds without the volume fraction correction
- Volume fraction correction resulted in a consistent and expected energy input

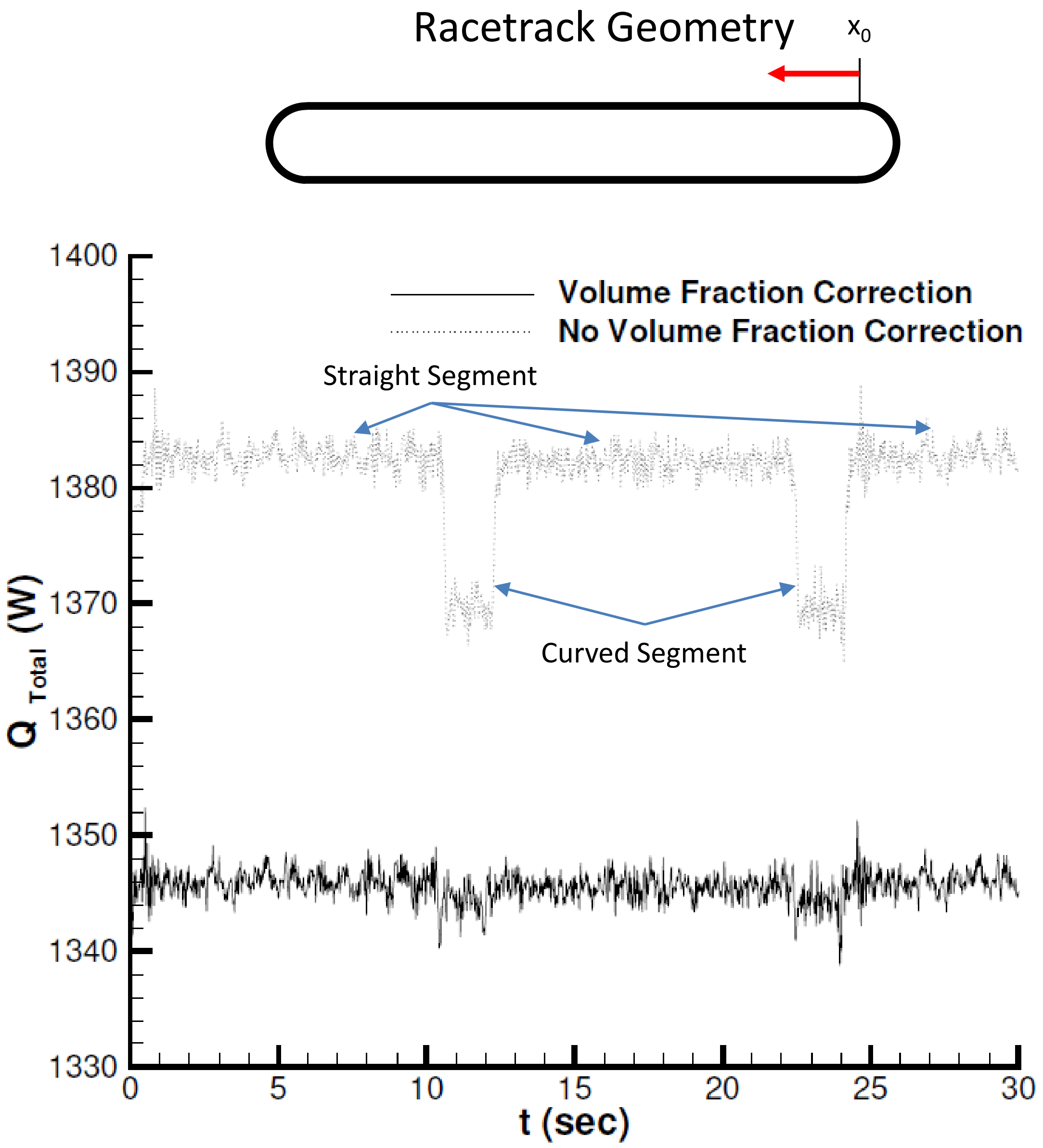

Phase Change Source

- Energy is released and absorbed due to melting/solidification and incorporated as a source term

$$S_p = -\rho L_f \frac{\partial f_L}{\partial t}$$

where L_f denotes the latent heat of fusion

- A continuous function is used to represent the liquid fraction (f_L) for numerical efficiency
- 99% of the energy change occurs between the solidus and liquidus temperatures

$\rho = 4428.7$ kg/m^3 $\quad T_S = 1877.6$ K

$L_f = 286$ kJ/kg $\quad T_L = 1933.2$ K

Liquid Fraction

$$f_L = \frac{1}{2}\left(1 + \mathrm{erf}\left(\frac{T - \mu_s}{\sigma_s\sqrt{2}}\right)\right)$$

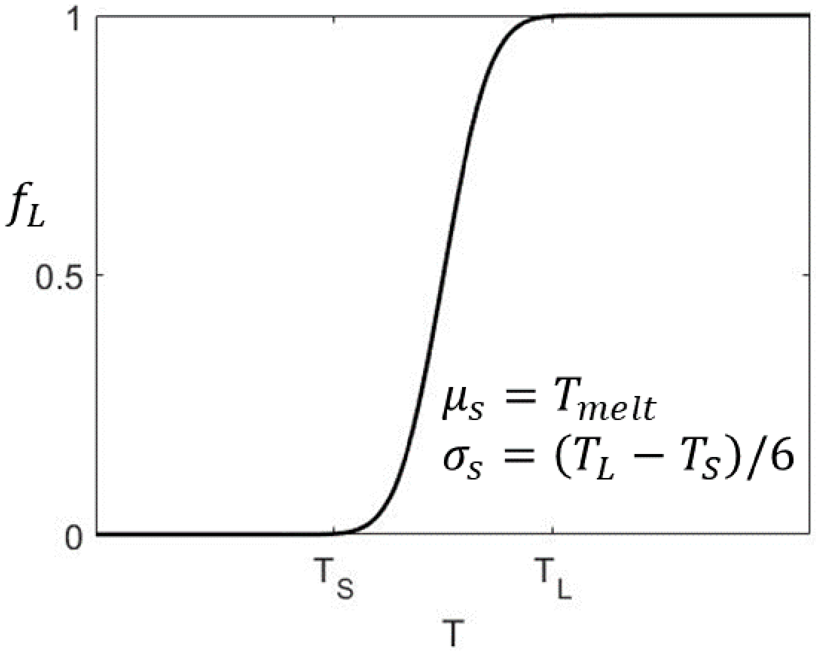

Electron Beam Heat Source

- Heat source parameters d, r_e, and r_i were manually perturbed until the predicted melt pool dimensions resulted in good agreement with the micrograph cross section images from the experimental welds
- Calibrated parameters:

$$d = 5.5 \text{ mm}, r_e = 2.0 \text{ mm},$$
$$r_i = 0.2 \text{ mm}$$

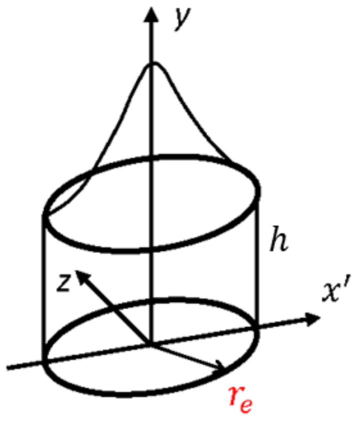

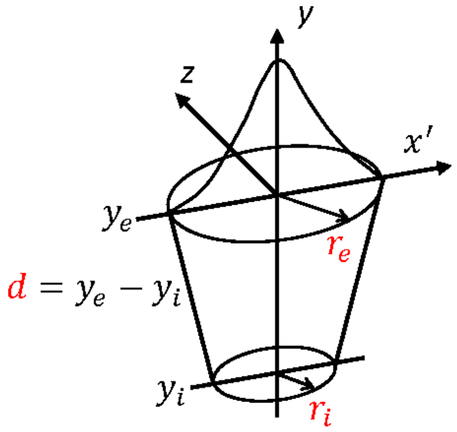

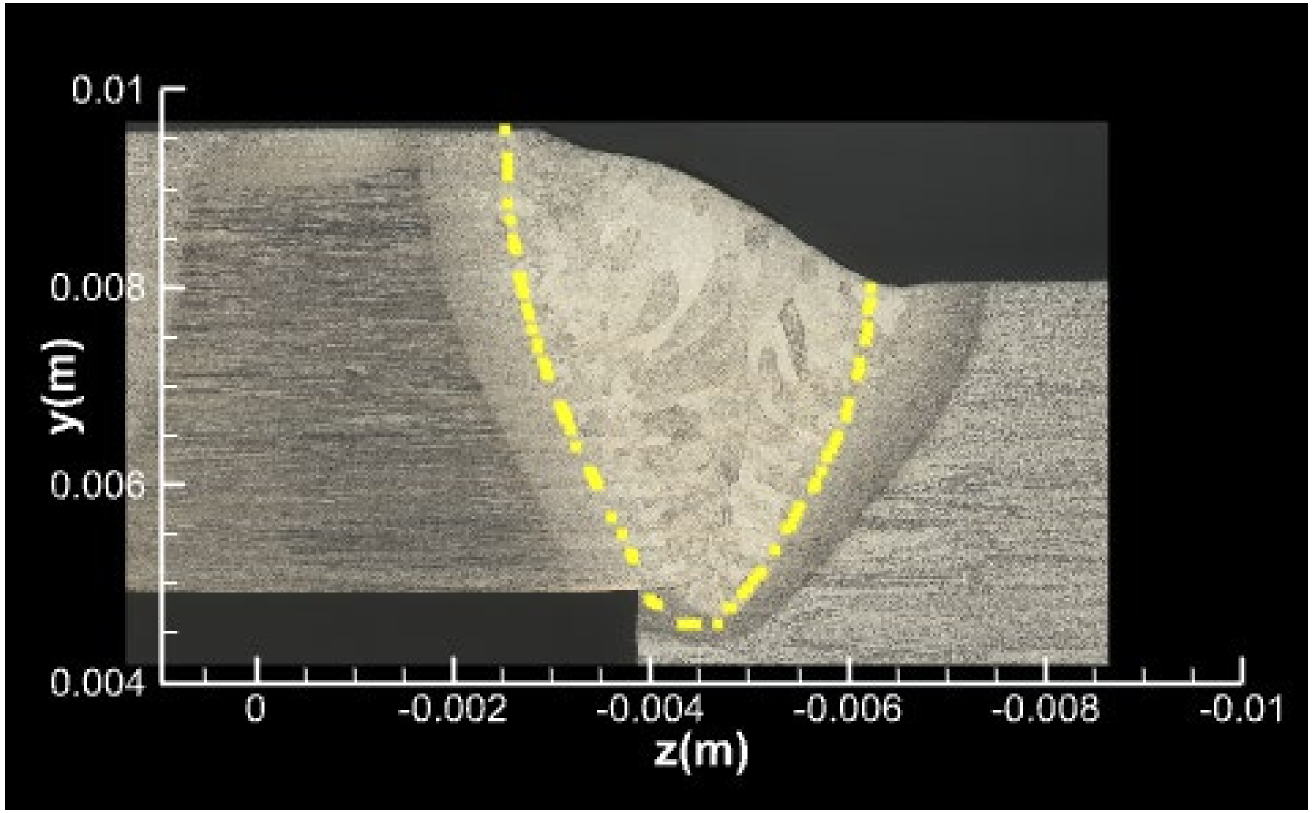

Cross-section micrograph image of weld trial with predicted melt interface in yellow

Process Induced Preheat

- Three values of interest were collected from the individual weld track models: melt pool width, melt pool depth, and process induced preheat (PIP)
- The PIP at a location along the heat source path is defined as the increase in temperature from the initial temperature, 298 K, directly before the heat source arrives

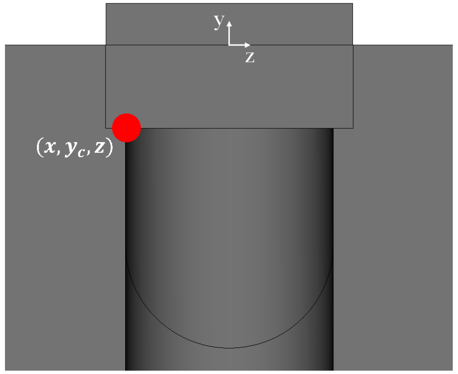

Location where the PIP is collected in individual weld track analysis

Racetrack Illustration

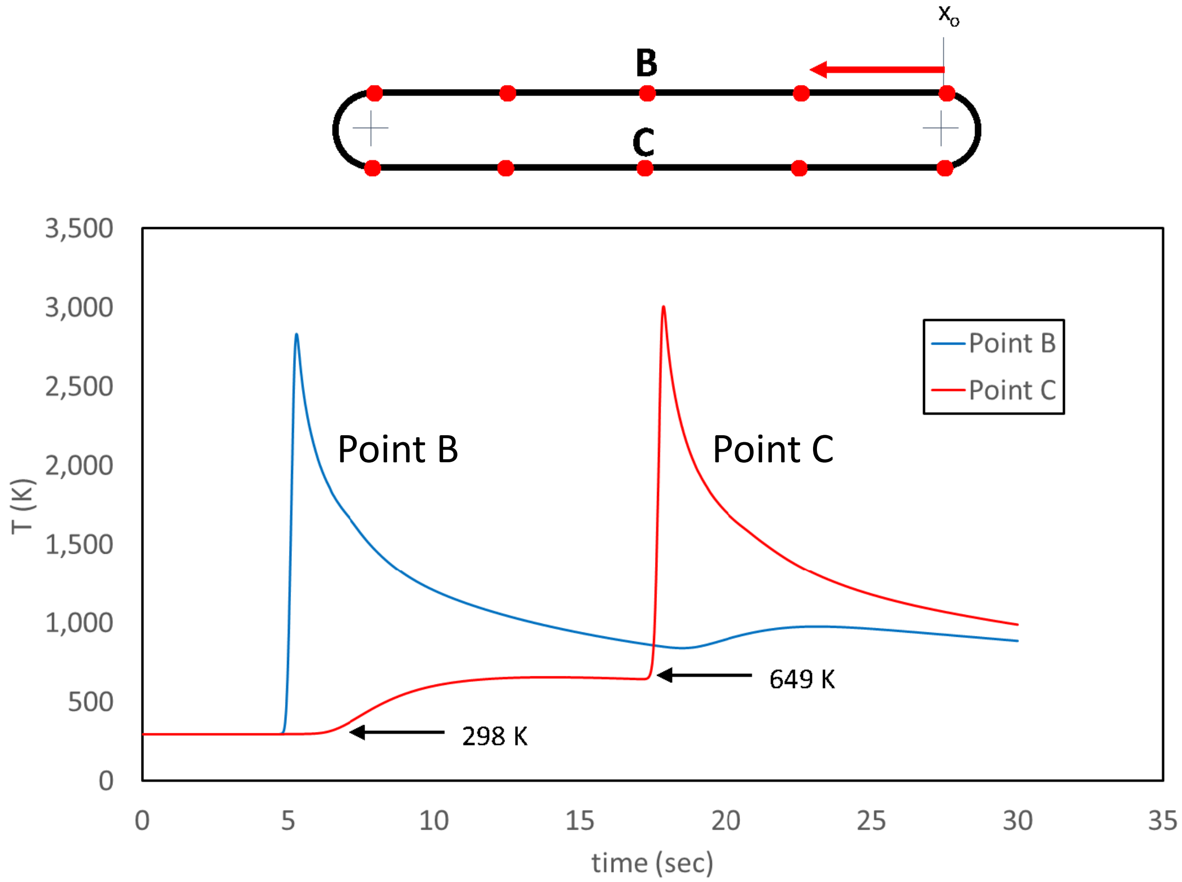

Temperature history at points B and C for the Racetrack
Point B: PIP = 0 K
Point C: PIP = 351 K

Results - Racetrack

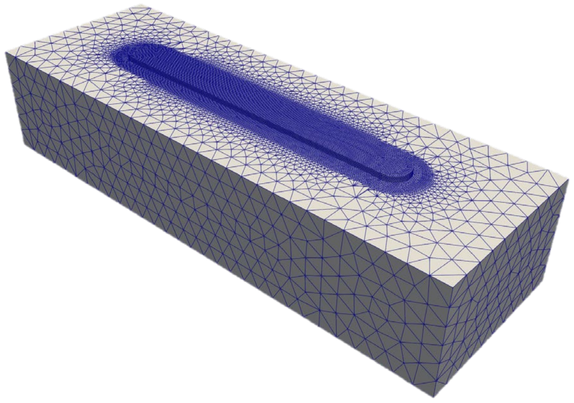

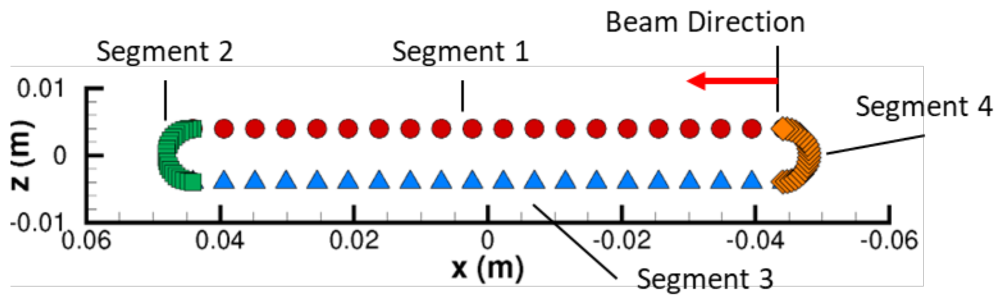

Racetrack analysis heat source position and segment markers

- PIP was zero in segment one
- Peak PIP occurred in segment three
- Peak was a result of:
  - Turn in segment two
  - Short amount of time between the heat source arriving at the same x-location in segments one and three
- The PIP increased during turn around segments

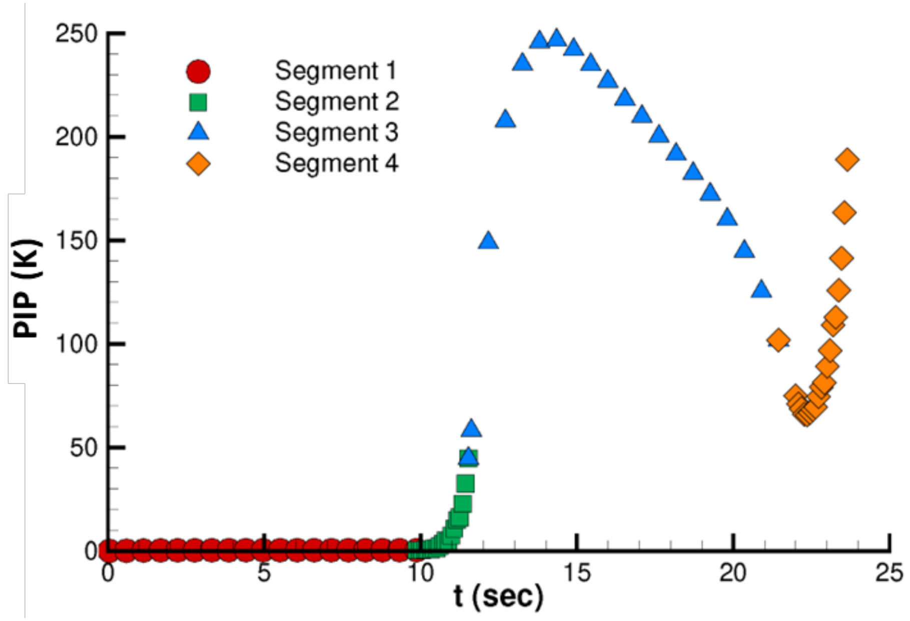

Racetrack analysis predicted PIP values

Results - Racetrack

- The predicted melt pool width increased in segments two and four where the PIP values increased
- A beam overlap occurred at the start of segment one leading to larger width and depth values

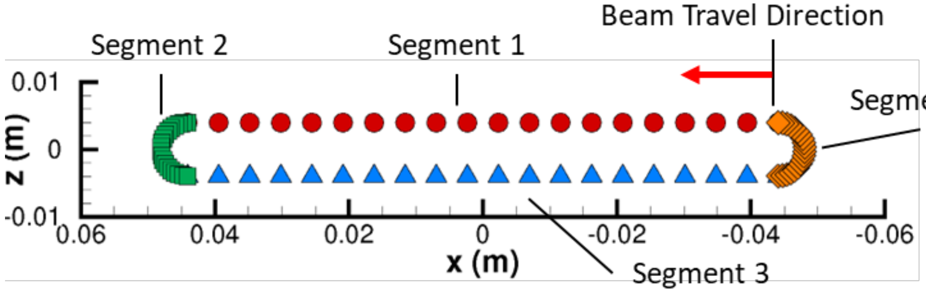

Racetrack analysis heat source position and segment markers

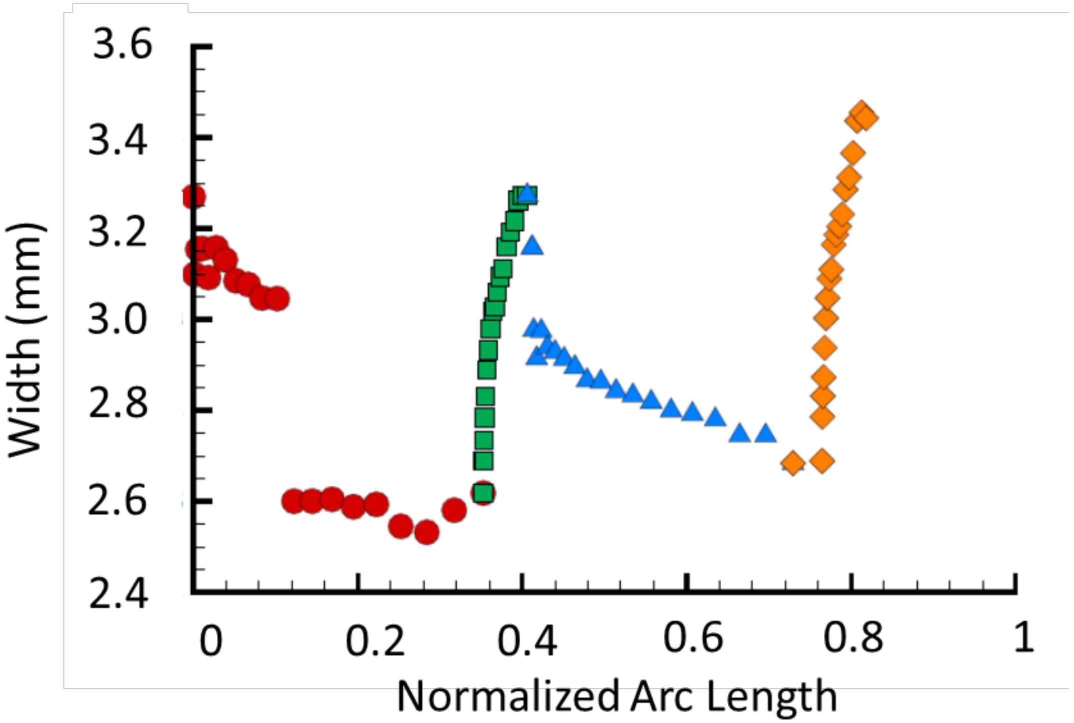

Racetrack analysis predicted width values

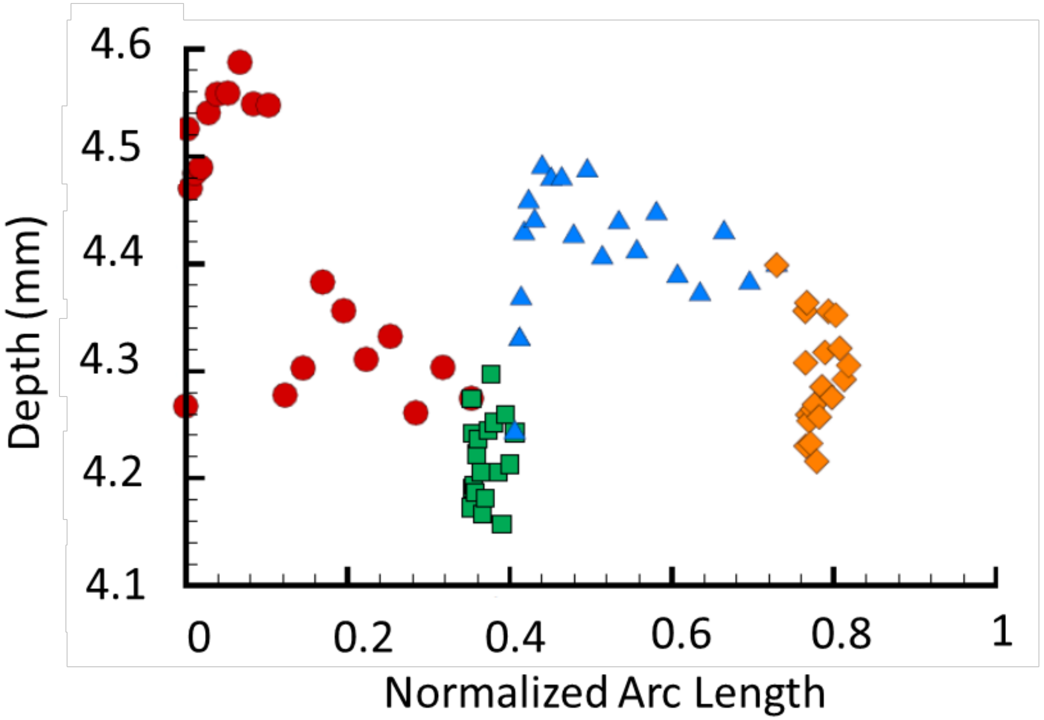

Racetrack analysis predicted depth values

Results – T-track

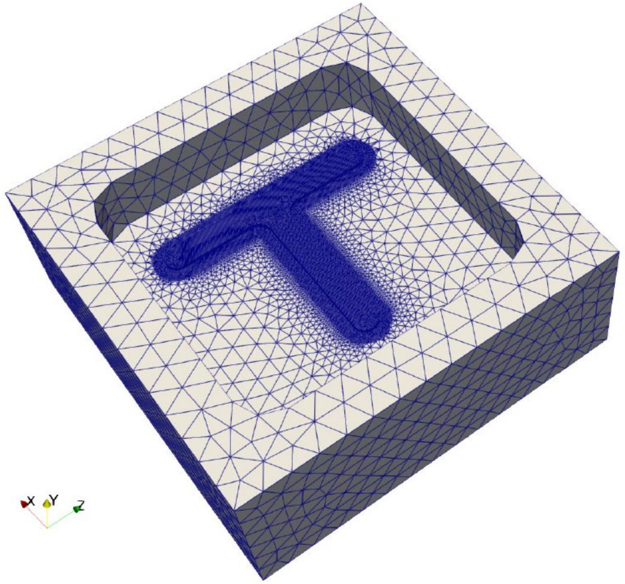

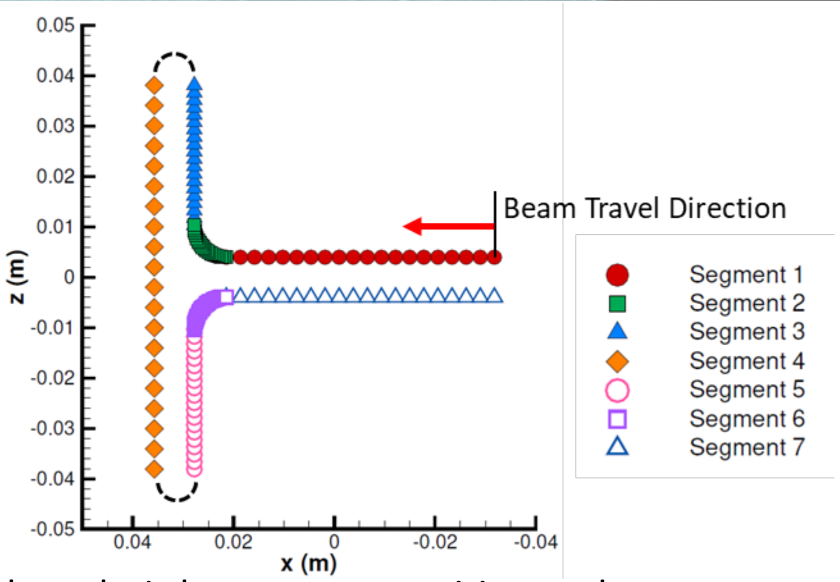

T-track analysis heat source position and segment markers

- Simulated pause times were included in the analysis at the turn-arounds (dashed lines)
- PIP was nearly zero in segment one through segment three
- Peak PIP occurred in segments four and six
- The peaks occur due to the short amount of time between the heat source location before and after the turns

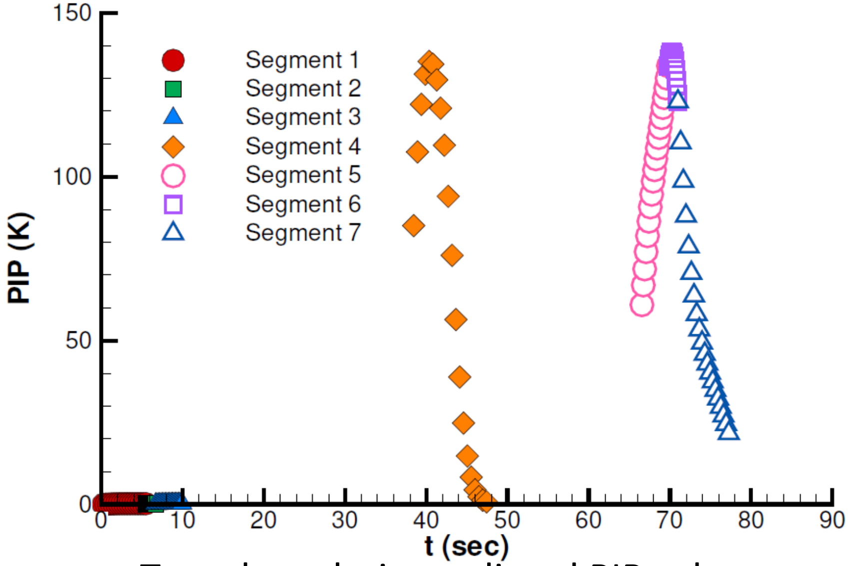

T-track analysis predicted PIP values

Results – T-track

- Predicted melt pool width increased in segments four through seven where PIP values were higher
- Predicted melt pool depth was consistent but increased in the turns, segments two and six

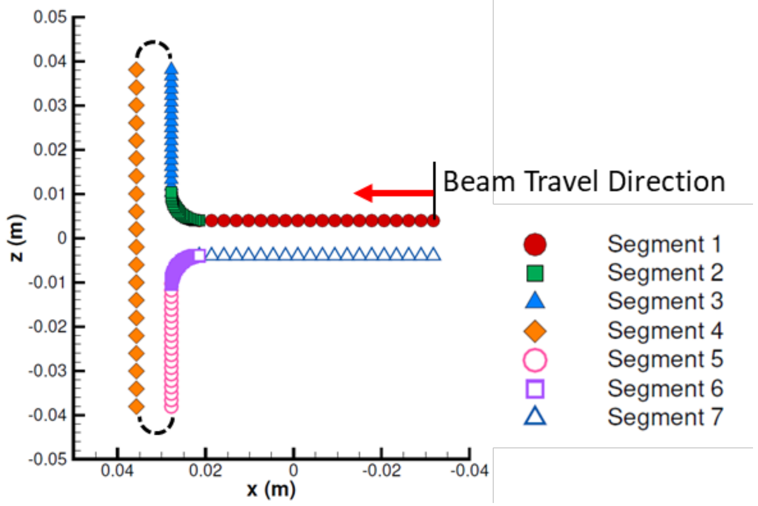

T-track analysis heat source position and segment markers

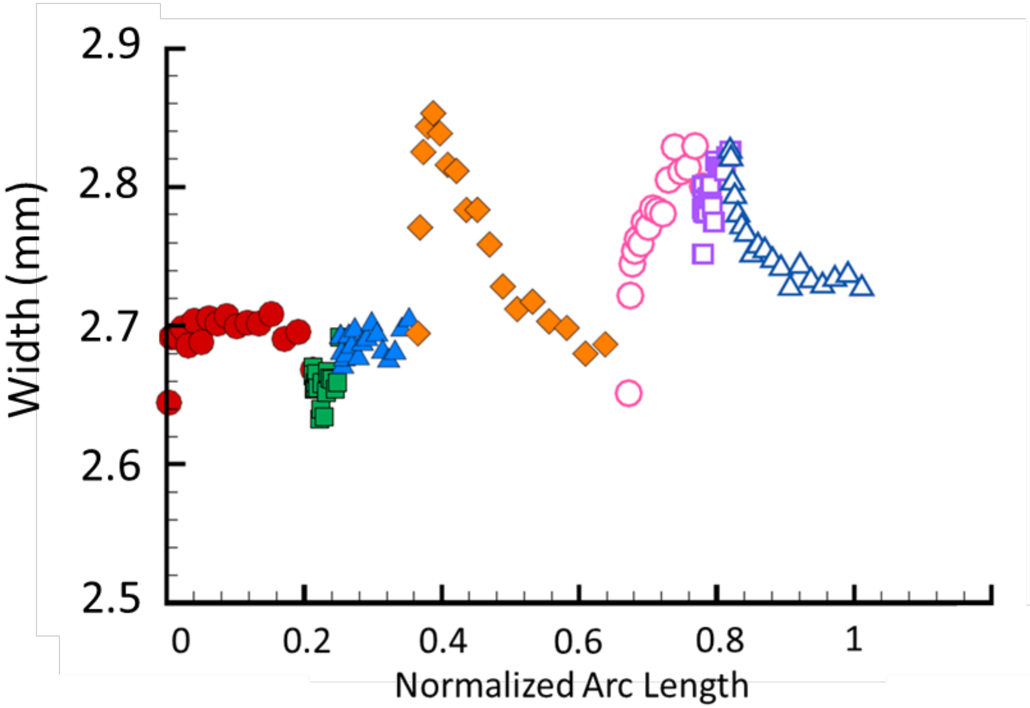

T-track analysis predicted width values

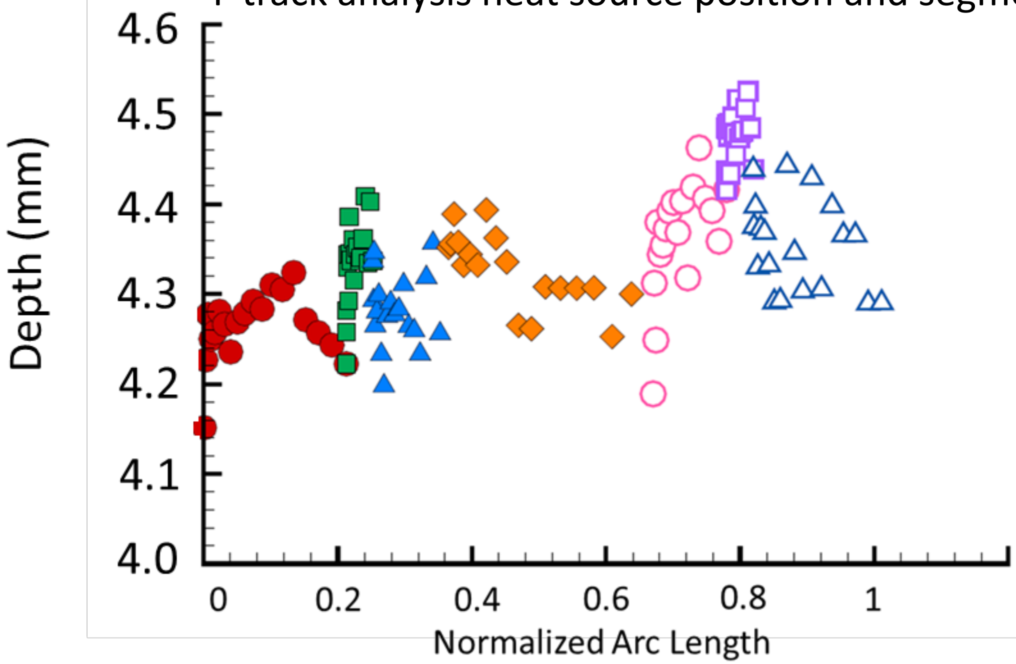

T-track analysis predicted depth values

T-track Weld Results

- T-track weld trial
  - No pause times at turn-arounds and constant weld parameters
  - Cross-sections generated at two locations
- Predicted peak PIP occurs at 17.5 mm from “ref”
- Predicted melt pool depths at section A agree with measured
- Decrease in melt intrusions along section B agree with PIP

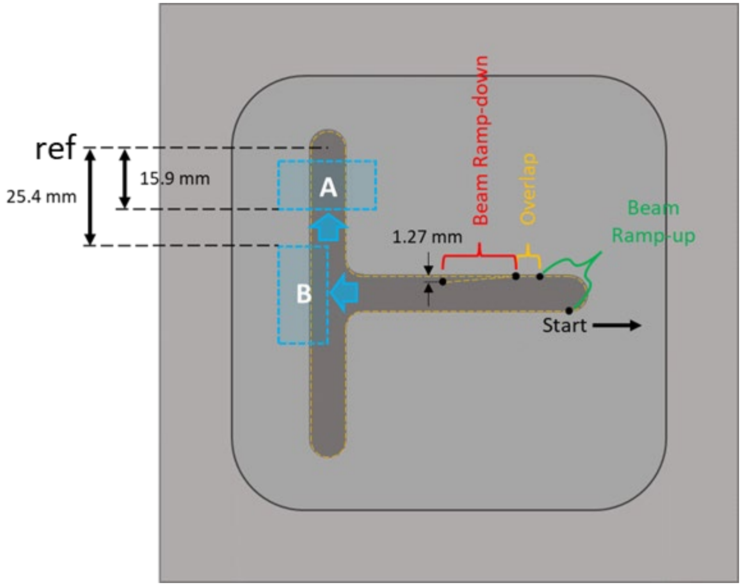

Beam position and cross-section locations

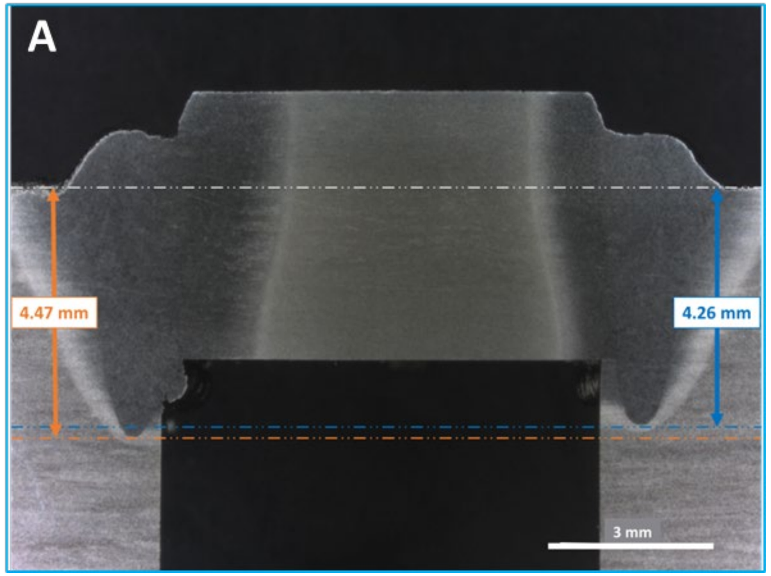

Cross-section at A

<u>Predicted Depth at A</u>
Minimum - 4.2 mm
Maximum - 4.4 mm

Cross-section at B

Results – Full-track

- The Full-track consists of all ten backplate weld tracks
- Various weld parameters were investigated to study interaction of weld tracks:
  - Pause times between welds
  - Weld sequence
  - Weld travel direction
- Channel and cover plate geometry were not included to allow analysis to run in a reasonable amount of time

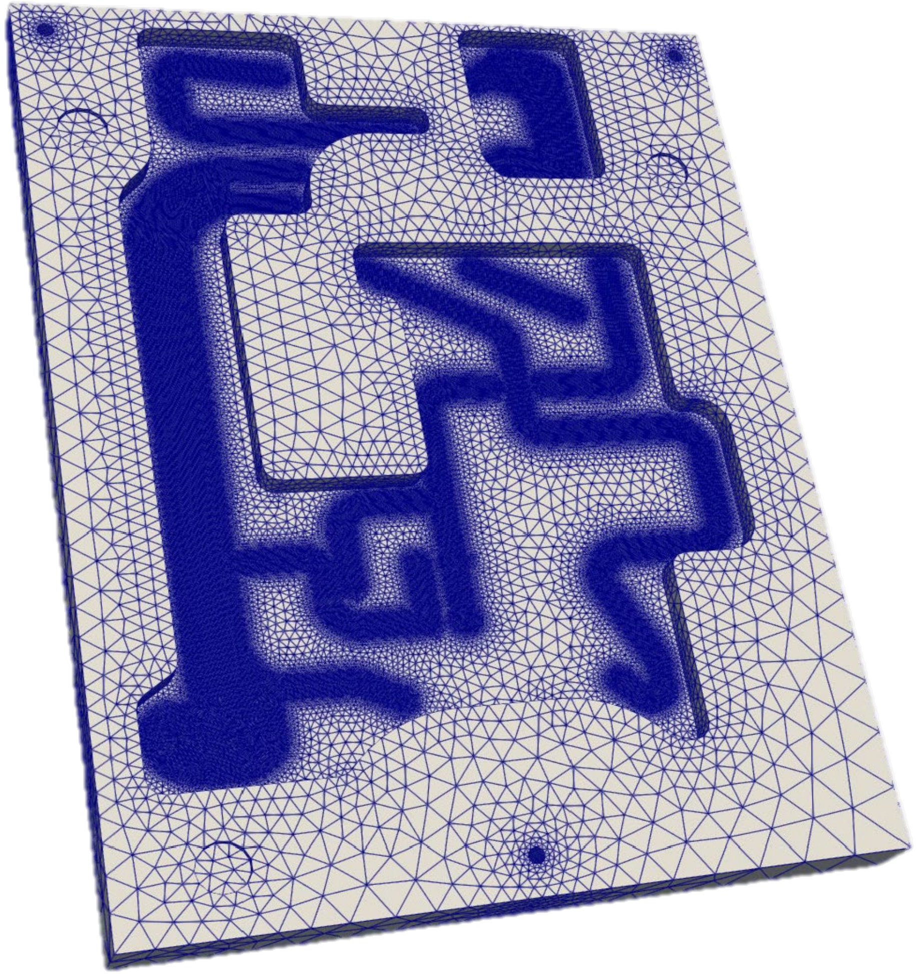

Full-track mesh

Results – Full-track

- Clockwise beam travel direction for all welds
- Starting locations are denoted by the blue triangles and peak PIP locations denoted by yellow circles
- Peak PIP values consistently occurred after a turn-around at the end of a channel
- Peak PIP values were consistent for all welds except weld track six whose peak PIP value was approximately 50 K higher

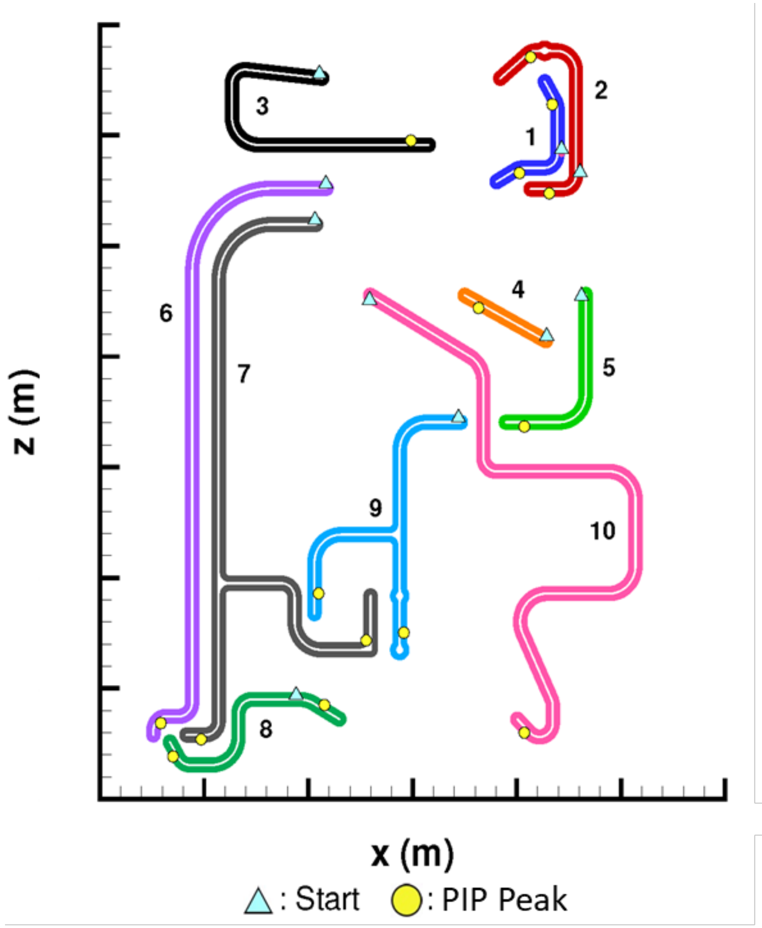

Full-track weld IDs with starting locations and predicted peak PIP locations

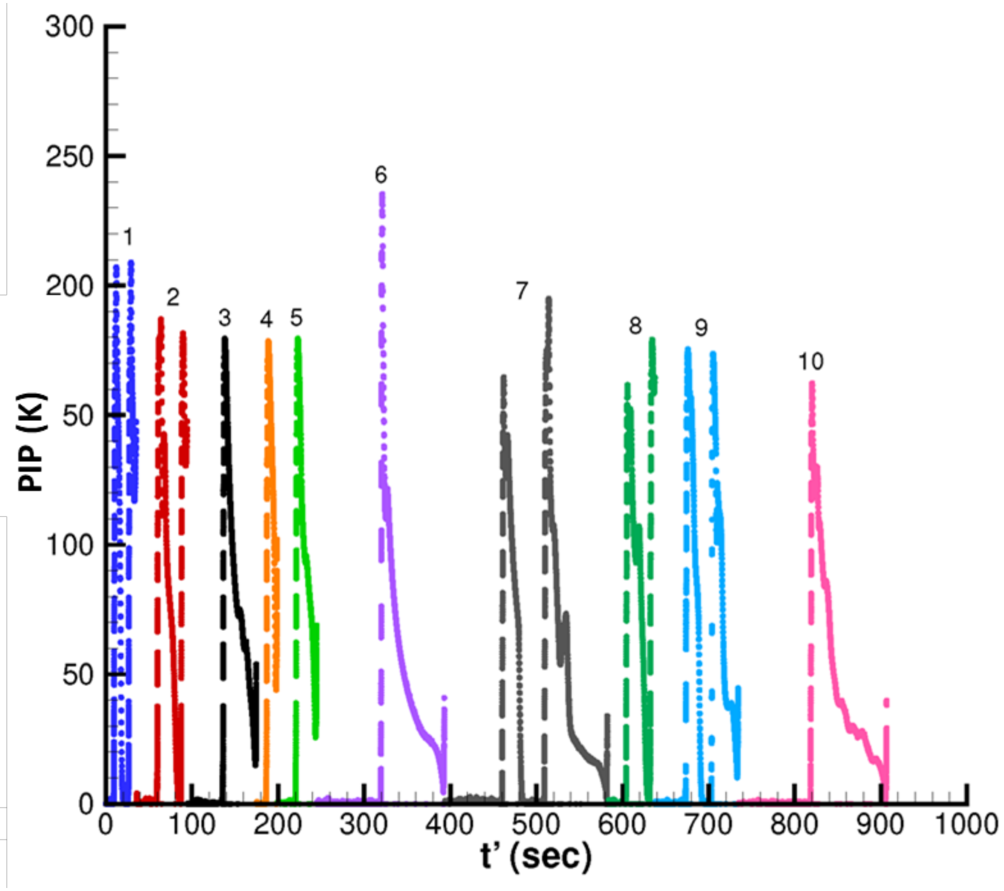

Full-track analysis predicted PIP values

Results - Weld Track Six

- The beam travel direction for weld track six was analyzed
- A counter-clockwise direction resulted in a peak PIP value of 235 K
- A clockwise direction resulted in a peak PIP value of 196 K
- A clockwise direction was implemented for weld track six in the backplate

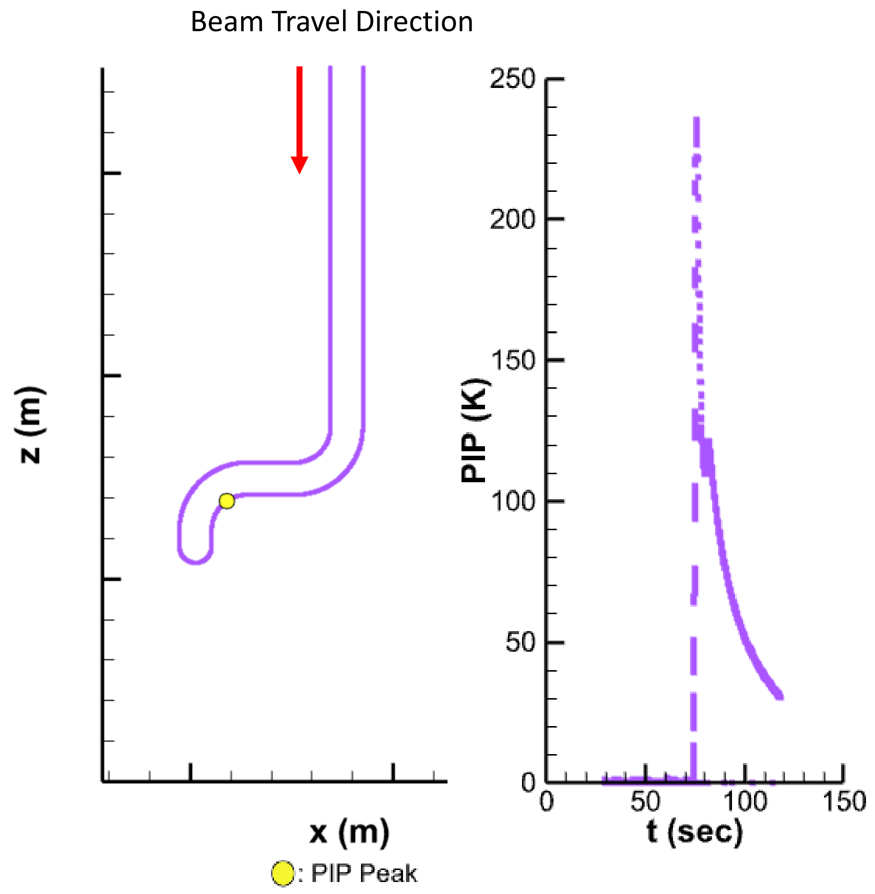

Heat source position and PIP values for a counter-clockwise beam travel direction

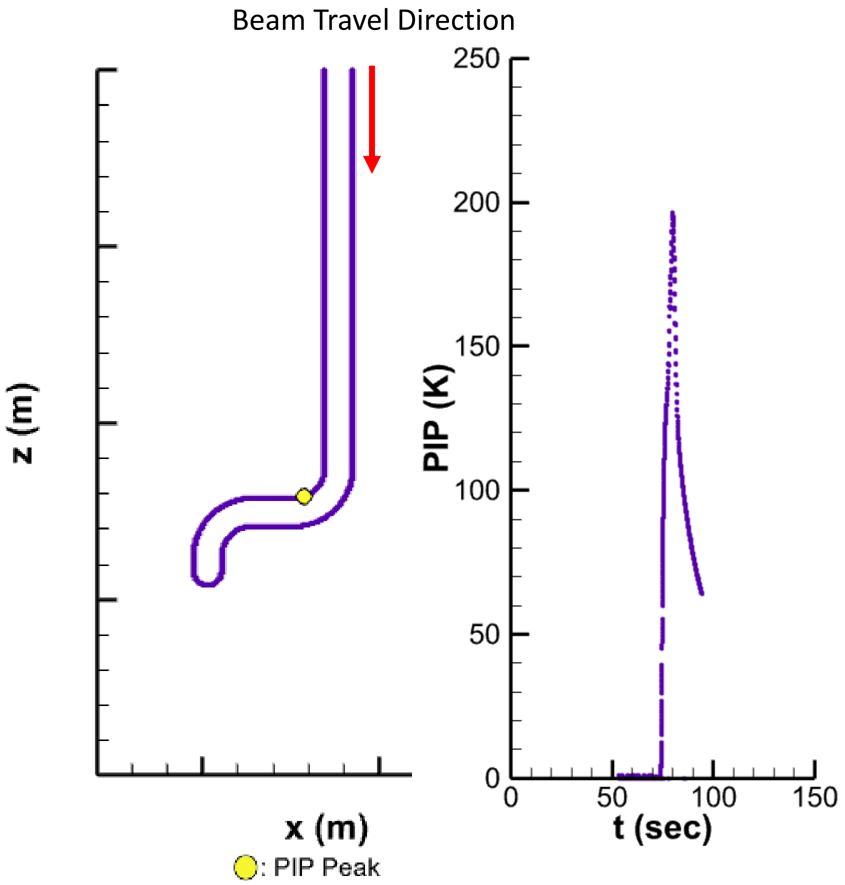

Heat source position and PIP values for a clockwise beam travel direction

Weld Track Six: Model to Weld Application

- Beam current (BC) is controlled according to predicted PIP

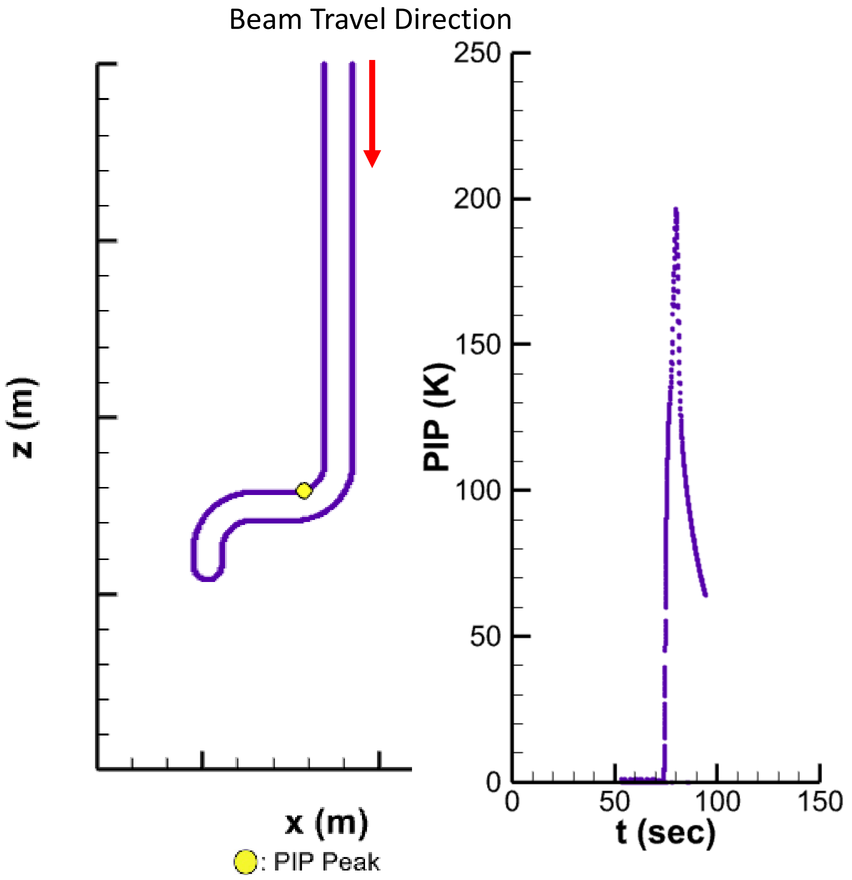

Heat source position and PIP values for a clockwise beam travel direction

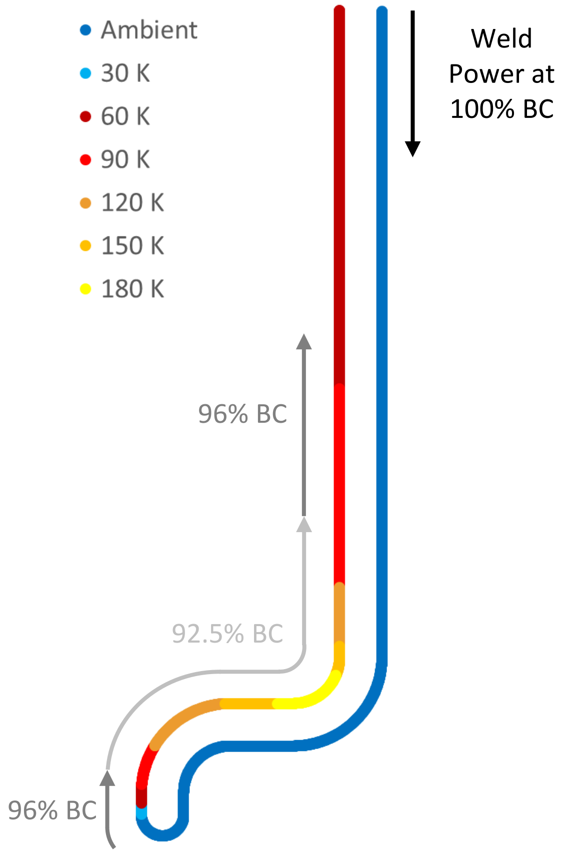

PIP depicted around weld path and the corresponding BC control

Weld track six imaged after electron beam welding

Concluding Remarks

What we completed

- Transient finite-element analyses were developed for the backplate welds of the next generation spacesuit
- A modified heat source was developed to accurately capture the total energy input
- The heat source parameters were calibrated to the melt interface from cross-section micrograph images
- Individual weld tracks and a full backplate with 10 channels were analyzed
- The analysis results were utilized in the weld process control to maintain a consistent melt pool shape
- Documented analysis work in project report and currently finalizing journal article submission

Concluding Remarks

What we learned

- Peak PIP values consistently occurred after a turn around at the end of a channel
- A beam travel direction change for weld track six from counter-clockwise to clockwise reduced the peak PIP by 40 K
- A ten-minute pause between weld tracks reduced the peak PIP up to 32 K as compared to no pauses
- The weld sequence had minimal impact on the magnitude and location of the predicted PIP peaks with ten-minute pauses

Impact of analysis work

- Analysis predictions were effective at tuning weld parameters to produce high quality welds
- Computational-based process control and adherence to strict weld protocols produced certifiable welds without 100% non-destructive inspection, which was challenging due to geometry
- Analysis calibration completed using Racetrack and T-track
- Successful weld of all backplate channels on first attempt
- Changes in channel geometry can be quickly accommodated

Thank you for your attention.